ARTICLE

Cyclic $M(SO_2)$ (M=Zn, Cd) and its Anions: Matrix Infrared Spectra and DFT Calculations†

Guang-jun Li, Xing Liu, Jie Zhao, Bing Xu, Xue-feng Wang*

Department of Chemistry, Key Laboratory of Yangtze River Water Environment, Ministry of Education, Tongji University, Shanghai 200092, China

(Dated: Received on October 30, 2013; Accepted on December 13, 2013)

Reaction of laser ablated zinc and cadmium atoms with SO_2 molecules was studied by low temperature matrix isolation infrared spectroscopy. Cyclic $M(SO_2)$ and anion $M(SO_2)^-$ (M=Zn, Cd) were produced in excess argon and neon, which were identified by $^{34}SO_2$ and $S^{18}O_2$ isotopic substitutions. The observed infrared spectra and molecular structures were confirmed by density functional theoretical calculations. Natural charge distributions indicated significant electron transfer from s orbitals of zinc or cadmium metal atom to SO_2 ligand and cyclic $M(SO_2)$ complexes favored "ion pair" $M^+(SO_2)^-$ formation, which were trapped in low temperature matrices. In addition Zn−O or Cd−O bond in $M(SO_2)$ exhibited strong polarized covalent character. Reaction of Hg atom with SO_2 was also investigated, but no reaction product was observed, due to the relativistic effect that resulted in the contraction of 6s valence shell and high ionization potential of Hg atom.

Key words: Sulfur dioxide, Matrix isolation, Transition metal, Density functional calculation

I. INTRODUCTION

Activation of S−O bond is of great interest due to the environmental implication for aerosols and acid rain [1−8]. The SO_2 molecule can be readily adsorbed on most pure metal and metal oxide surfaces to form complexes, which is the first step toward S−O bond breaking. The first complexes of sulfur dioxide, *trans*-$[Ru(X)(NH_3)_4(SO_2)]^+$ (X=Cl, Br) and *trans*-$[Ru(L)(NH_3)_4(SO_2)]_2^+$ (L=H_2O, NH_3), were synthesized in 1938 [9, 10]. Since then many sulfur dioxide compounds of transition metals (d-group) [11−16], lanthanides (f-group) [17, 18], and alkali and alkaline earth metals (s-group) [19−21] have been prepared. Recently molecular SO_2 complexes of lanthanides were prepared and bridged M−O−S−O−M structures were identified [22]. So far five common types of metal-SO_2 complexes have been reported, which are coplanar η^1-S, pyramidal, η^2-O,S-bonded complexes, η^1-O fashion, and ionic complexes [13, 23].

Recently, reactions of transition atom with SO_2 have been studied in low temperature matrices, and metal sulfide oxides SMO_2 (Cr, Mo, W), anion SMO_2^- (M=V, Nb, Ta), and complexes $OM(\eta^2$-SO) (M=Ti, Zr, Hf) have been identified [6, 24, 25]. In this work the reactions of laser-ablated zinc, cadmium and mercury atoms with SO_2 in solid neon and argon were performed and infrared spectra were used to collect molecular vibrational information. The experimental data were reproduced by the density functional theory (DFT) theoretical calculations. The nature of bonding was discussed based on the natural charge distribution and the electronic population analysis.

II. EXPERIMENTS AND COMPUTATIONAL METHODS

The experimental methods and apparatus for investigating laser ablated transition metal atom reactions with small molecules during condensation in excess neon at 5 K have been described in our previous work [24−26]. The Nd:YAG laser fundamental (1064 nm, 10 Hz repetition rate with 10 ns pulse width) was focused onto a rotating metal target, which then gave a bright plume spreading uniformly to the cold CsI window. The zinc and cadmium targets were polished to remove oxide coating and immediately placed in the vacuum chamber. Liquid mercury was stored in a sealed tube, which was evaporated slightly above room temperature to give Hg atoms. We also tried to put 10%Na to liquid Hg to form solid amalgam, which was ready to laser ablation. A mixture of $S^{18}O_2$ and $S^{16,18}O_2$ with trace of $S^{16}O_2$ was prepared by tesla coil discharge of $^{18}O_2$ (>99%, Shanghai Research Institute of Chemical Industry) (about 2 Torr) in a 0.5 L pyrex bulb containing 10 mg of sulfur powder (99.5%, Alfa Ae-

†Part of the special issue for "the Chinese Chemical Society's 13th National Chemical Dynamics Symposium".

*Author to whom correspondence should be addressed. E-mail: xfwang@tongji.edu.cn

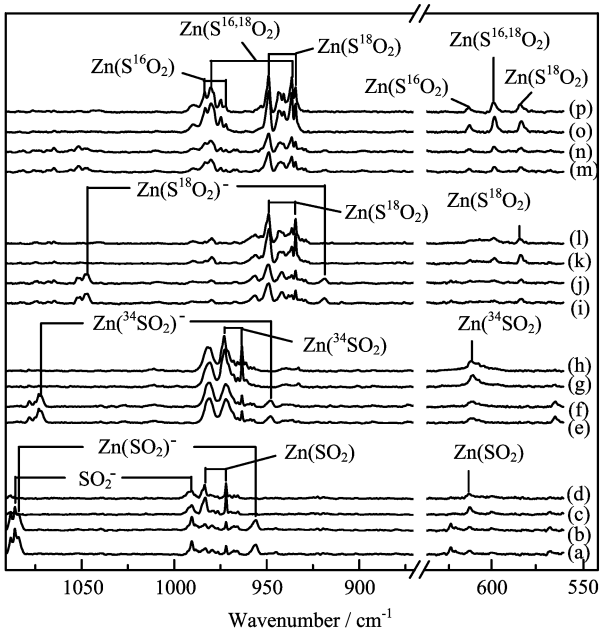

FIG. 1 Infrared spectra for the Zn atom and SO_2 reaction products in solid neon at 5 K. (a) Zn+SO_2 deposition for 60 min, (b) after annealing to 8 K, (c) after full-arc irradiation for 15 min, (d) after annealing to 10 K; (e) Zn+$^{34}SO_2$ deposition for 60 min, (f) after annealing to 8 K, (g) after full-arc irradiation for 15 min, (h) after annealing to 10 K; (i) Zn+$S^{18}O_2$ deposition for 60 min, (j) after annealing to 8 K, (k) after full-arc irradiation for 15 min, (l) after annealing to 10 K; (m) Zn+$S^{16,18}O_2$ deposition for 60 min, (n) after annealing to 8 K, (o) after full-arc irradiation for 15 min, (p) after annealing to 10 K.

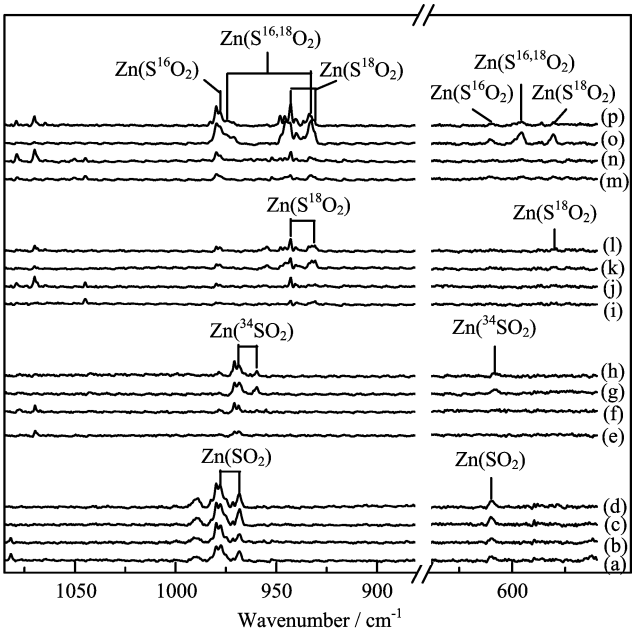

FIG. 2 Infrared spectra for the Zn atom and SO_2 reaction products in solid argon at 5 K. (a) Zn+SO_2 deposition for 60 min, (b) after annealing to 20 K, (c) after full-arc irradiation for 15 min, (d) after annealing to 35 K; (e) Zn+$^{34}SO_2$ deposition for 60 min, (f) after annealing to 20 K, (g) after full-arc irradiation for 15 min, (h) after annealing to 35 K; (i) Zn+$S^{18}O_2$ deposition for 60 min, (j) after annealing to 20 K, (k) after full-arc irradiation for 15 min, (l) after annealing to 35 K; (m) Zn+$S^{16,18}O_2$ deposition for 60 min, (n) after annealing to 20 K, (o) after full-arc irradiation for 15 min, (p) after annealing to 35 K.

sar) sublimed onto the walls heated by external hot air (>450 °C). The sample of $^{34}SO_2$ was similarly prepared from sulfur-34 (98.8%, ^{34}S, Cambridge Isotope Laboratories) and oxygen (99.999%, British Oxygen Company). The laser energy was varied in the range of 10−20 mJ/pulse. FTIR spectra were recorded at 0.5 cm^{-1} resolution on a Bruker Vertex 80 V with 0.1 cm^{-1} accuracy using an MCTB detector. The co-deposited samples were annealed at different temperatures, and selected samples were subjected to irradiation by a medium pressure mercury arc lamp (Philips, 175 W).

Density functional theory calculations were done to get the anticipated products with the use of the Gaussian 03 program [27], the B3LYP functional, the 6-311++G(3df, 3pd) basis set for sulfur and oxygen atoms, and the SDD pseudo potential for zinc, cadmium, and mercury [28−33]. Different spin states were also explored to locate the ground state product molecules. All of the geometrical parameters were fully optimized and harmonic vibrational frequencies were calculated analytically with the optimized configurations. The BPW91 functional was processed to support the computational results. Meanwhile, the CCSD(T) functional was adopted to conduct the energy correction for the optimized molecules.

III. RESULTS

Laser ablated zinc and cadmium reacted with SO_2 in excess neon and argon. The products were detected by FTIR spectra. Similar experiments were done for mercury atom reaction with SO_2, however, no reaction products were observed. DFT frequency calculations were performed to reproduce the observed absorptions and the chemical bonding for the complexes was discussed based on natural charge distribution and the electronic population analysis.

A. Zn+SO_2/Ne and Zn+SO_2/Ar

As shown in Fig.1 laser ablated Zn atom reactions with SO_2 in neon gave three weak bands at 983.5, 972.0, and 612.8 cm^{-1} (group 1) and two stronger bands at 1083.9 and 956.1 cm^{-1} (group 2). These two groups of absorptions changed scarcely after annealing to 8 K. UV light irradiation further increased all bands of group 1, but destroyed the features of group 2 bands. The group

DOI:10.1063/1674-0068/26/06/747-754

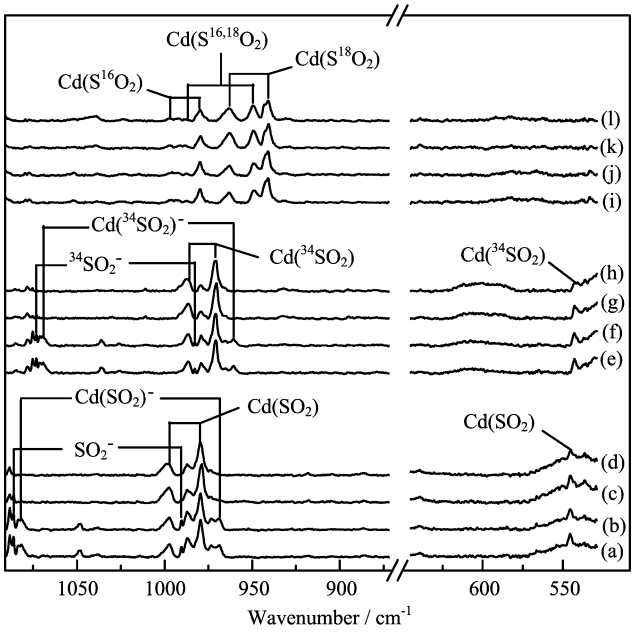

FIG. 3 Infrared spectra for the Cd atom and SO_2 reaction products in solid neon at 5 K. (a) Cd+SO_2 deposition for 60 min, (b) after annealing to 8 K, (c) after full-arc irradiation for 15 min, (d) after annealing to 10 K; (e) Cd+$^{34}SO_2$ deposition for 60 min, (f) after annealing to 8 K, (g) after full-arc irradiation for 15 min, (h) after annealing to 10 K; (i) Cd+$S^{16,18}O_2$ deposition for 60 min, (j) after annealing to 8 K, (k) after full-arc irradiation for 15 min, (l) after annealing to 10 K.

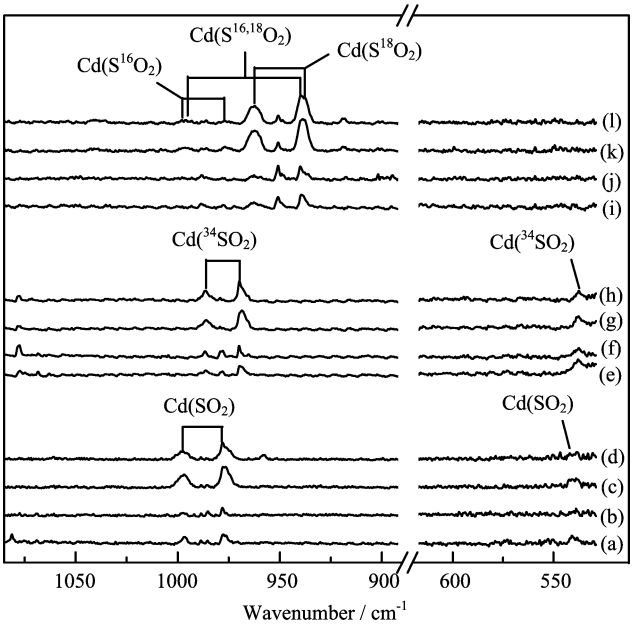

FIG. 4 Infrared spectra for the Cd atom and SO_2 reaction products in solid argon at 5 K. (a) Cd+SO_2 deposition for 60 min, (b) after annealing to 20 K, (c) after full-arc irradiation for 15 min, (d) after annealing to 35 K; (e) Cd+$^{34}SO_2$ deposition for 60 min, (f) after annealing to 20 K, (g) after full-arc irradiation for 15 min, (h) after annealing to 35 K; (i) Cd+$S^{16,18}O_2$ deposition for 60 min, (j) after annealing to 20 K, (k) after full-arc irradiation for 15 min, (l) after annealing to 35 K.

1 bands slightly decreased on further annealing to 10 K. Similar profiles were also obtained in the argon matrix experiment (Fig.2). The photosensitive bands (group 2) were so weak that they were hardly observed while corresponding group 1 bands were observed at 977.8, 968.6, and 610.7 cm^{-1}.

B. Cd+SO_2/Ne and Cd+SO_2/Ar

Figure 3 shows the product absorptions for laser ablated cadmium atom reactions with SO_2 in excess neon. Group 1 bands at 997.4, 979.6, and 545.6 cm^{-1} were observed on deposition, decreased slightly on annealing to 8 K and enhanced by 30% on further UV irradiation. Another two weak features at 1081.7 and 969.3 cm^{-1} (group 2) were also observed on deposition but disappeared on UV irradiation. The corresponding bands in solid argon matrix are shown in Fig.4. New adsorptions at 996.9, 977.9, and 542.1 cm^{-1} were tremendously increased on full-arc irradiation, and decreased 50% on further annealing to 10 K.

C. Calculations

The structures of M(SO_2) and M$(SO_2)^-$ complexes (M=Zn, Cd, Hg) have been optimized with B3LYP and BPW91 functional and the calculated structure parameters are given in Fig.5. The η^2-O,O bonded cyclic Zn(SO_2) complex is located the lowest on triplet potential energy surface (Fig.6) while η^1-S bonded Zn(SO_2) complex is around 27.6 kcal/mol higher at the same level calculation. Similar energy profiles were obtained for cadmium and mercury with SO_2 complexes. The η^1-O bonded fashion was found for all three M$(SO_2)^-$ anions. The calculated frequencies for all stable molecules are listed in Tables II−III. Natural charge distributions and natural electron configuration are listed in Tables IV and V.

IV. DISCUSSION

A. Cyclic M(SO_2) (M=Zn, Cd)

In the experiments with laser-ablated zinc atom reactions with sulfur dioxide during condensation in solid neon, three bands at 983.5, 972.0, and 612.8 cm^{-1} track together, suggesting that this group bands are due to the same molecule. In the ^{18}O isotopic experiment, the counterpart bands were found at 949.0, 934.4, and 583.7 cm^{-1} with 1.0363, 1.0402, and 1.0499 $^{16}O/^{18}O$ isotopic ratios. In the same experiment with mixed $^{16}O/^{18}O$ sample triplet oxygen isotopic distributions were observed for three bands, indicating the involve-

DOI:10.1063/1674-0068/26/06/747-754

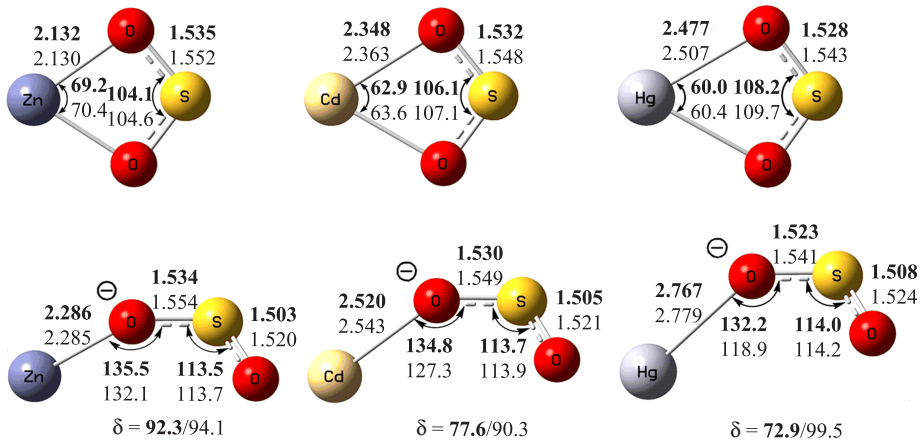

FIG. 5 Calculated structure for molecules of Zn, Cd, and Hg combined with SO_2 based on B3LYP (in bold) and BPW91 functional calculations (bond lengths in Å and bond angles in (°), δ is dihedral angle in (°)).

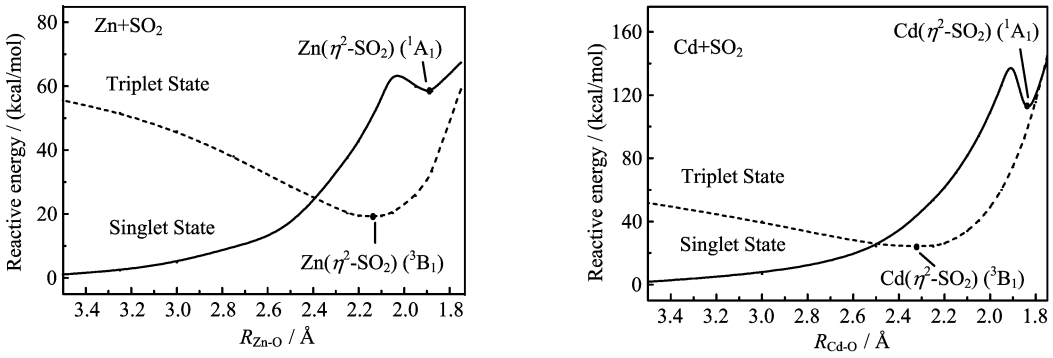

FIG. 6 Singlet and triplet PES for Zn+SO_2 and Cd+SO_2 based on B3LYP functional calculation (R is the distance between metal and oxygen).

ment of two equivalent oxygen atoms for each mode. Since three bands shift to 973.0, 963.4, and 611.2 cm^{-1} with ^{34}S enriched sample, the participation of sulfur atom is confirmed. The 983.5 and 972.0 cm^{-1} bands are located in S−O single bond stretching region and 612.8 cm^{-1} band is due to O−S−O bending mode, so $Zn(SO_2)$ molecule is proposed. In solid argon matrix, counterpart bands were observed at 977.8, 968.6, and 610.7 cm^{-1}. This is further substantiated by the observation of three fundamentals at 942.9, 930.8, and 580.9 cm^{-1} with ^{18}O substituted sample and one extra absorption for each mode in the intermediate region with $SO_2/S^{16,18}O_2/S^{18}O_2$ mixture. With $^{34}SO_2$ sample three counterpart bands were found at 968.8, 959.8, and 607.5 cm^{-1}. Notice the upper 983.5 cm^{-1} band is broader, which is probably due to higher complex bands overlapped.

Our DFT (B3LYP) calculation predicts the O−S−O bond angle in triplet $Zn(\eta^2\text{-}O_2S)$ as 104.1°, which is much smaller than 119.2° for singlet SO_2 calculated at the same level, suggesting strong bonding between Zn and SO_2. The S=O antisymmetric and symmetric stretching modes are computed at 980.7 and 978.6 cm^{-1}, which are within 99% accuracy compared with neon values. In addition, the calculated isotopic frequencies for S-34 and O-18 substitutions match the observed values very well.

Laser ablated cadmium atom reactions with SO_2 in solid neon gave three bands at 997.4, 979.6, and 545.6 cm^{-1}. With ^{18}O enriched sample the former two bands shifted to 963.0 and 940.8 cm^{-1}, respectively, giving 1.0357 and 1.0412 $^{16}O/^{18}O$ isotopic frequency ratios. As shown in Fig.3, there is about $15\%SO_2+30\%S^{16,18}O_2+55\%S^{18}O_2$ in the sample triplet oxygen isotopic distributions, which were observed for stronger 997.4 and 979.6 cm^{-1} band, indicating the participation of two oxygen atoms for this mode. With $^{34}SO_2$ enriched sample these bands shift to 986.5, 970.6, and 542.9 cm^{-1}, respectively, suggesting sulfur atom involvement in these vibrations. Based on above spectrum features this group bands are appropriate $Cd(SO_2)$ complex.

Our DFT calculations strongly support the assignments. The cyclic $Cd(SO_2)$ molecule was calculated to be $^3B_1$ ground state with C_{2v} structure, and symmetric and antisymmetric S−O stretching vibrational modes are predicted at 976.1 and 985.2 cm^{-1} with B3LYP calculation, which are underestimated by 0.4% (symmetric

DOI:10.1063/1674-0068/26/06/747-754

TABLE I Infrared absorptions (in cm^{-1}) observed for products of the reaction of Zn and Cd atoms with SO_2 molecules in neon and argon.

	$^{32}S^{16}O_2$	$^{34}S^{16}O_2$	$^{32}S^{16,18}O_2$+$^{32}S^{18}O_2$	Ratio ($^{16}O/^{18}O$)	Identity
Zn (Ne)	983.5	973.0	985.0, 949.0	1.0363	Zn(η^2-O_2S)
	972.0	963.4	936.6, 934.4	1.0402	Zn(η^2-O_2S)
	612.8	611.2	598.5, 583.7	1.0499	Zn(η^2-O_2S)
	1083.9	1071.7	1081.4, 1046.8	1.0346	Zn(η^1-OSO)$^-$
	956.1	948.0	918.9	1.0405	Zn(η^1-OSO)$^-$
Zn (Ar)	977.8	968.8	974.6, 942.9	1.0370	Zn(η^2-O_2S)
	968.6	959.8	932.8, 930.8	1.0406	Zn(η^2-O_2S)
	610.7	607.5	595.9, 580.9	1.0513	Zn(η^2-O_2S)
Cd (Ne)	997.4	986.5	992.5, 963.0	1.0357	Cd(η^2-O_2S)
	979.6	970.6	949.4, 940.8	1.0412	Cd(η^2-O_2S)
	545.6	542.9			Cd(η^2-O_2S)
	1081.7	1069.4	1077.6		Cd(η^1-OSO)$^-$
	969.3	961.0			Cd(η^1-OSO)$^-$
Cd (Ar)	996.9	985.3	994.6, 962.5	1.0357	Cd(η^2-O_2S)
	977.9	968.7	940.0, 938.8	1.0416	Cd(η^2-O_2S)
	542.1	538.6			Cd(η^2-O_2S)

TABLE II Calculated frequencies of cyclic $M(SO_2)$ complexes (M=Zn and Cd) molecule[a].

	B3LYP				BPW91	Mode description
	^{16}O	^{16}O, ^{18}O	^{18}O	^{16}O, ^{34}S	^{16}O	
Zn(η^2-O_2S)	980.7(134)	979.6(108)	946.4(125)	970.1(75)	935.6(108)	S−O antisym str
	978.6(77)	943.1(96)	939.7(72)	969.5(132)	927.8(58)	S−O sym str
	553.0(57)	540.1(53)	527.0(48)	549.9(59)	520.9(47)	S−O sciss
	281.5(37)	277.5(36)	275.4(36)	277.0(35)	271.6(31)	OSO rock
	212.2(10)	207.9(10)	203.8(9)	210.2(10)	205.6(9)	OSO wag
	172.2(11)	167.4(10)	163.3(10)	171.8(11)	170.5(9)	OSO def
Cd(η^2-O_2S)	985.2(140)	981.4(115)	951.4(129)	973.8(137)	942.2(112)	S−O antisym str
	976.1(71)	943.4(88)	937.0(66)	967.8(69)	926.1(48)	S−O sym str
	533.9(46)	521.7(42)	509.1(39)	530.9(48)	502.0(35)	S−O sciss
	229.1(29)	227.8(29)	225.6(28)	227.4(28)	218.7(23)	OSO rock
	199.6(11)	195.9(10)	192.0(10)	197.9(11)	193.3(9)	OSO wag
	168.0(10)	163.5(9)	159.3(9)	168.1(9)	169.2(8)	OSO def

[a] Frequencies in cm^{-1}, intensities (in parentheses) in km/mol.

mode) and by 1.2% (antisymmetric mode), respectively. Similar frequency calculations for cyclic $Cd(SO_2)$ with BPW91 giving 926.1 and 942.2 cm^{-1} for both symmetric and antisymmetric SO stretching modes are almost underestimated by 5.8% and 5.9%.

The reaction of zinc atom with SO_2 to give cyclic $Zn(SO_2)$ is endothermic (ZPE correction included) by 13 kcal/mol based on CCSD(T) calculation (Reaction (1)). Similar endothermic energy is predicted for formation of cyclic $Cd(SO_2)$ (Reaction (2)).

$$\mathrm{Zn} + \mathrm{SO_2} \xrightarrow{\mathrm{UV}} \text{cyclic } \mathrm{Zn(SO_2)}$$
$$\Delta E = 13 \text{ kcal/mol} \quad (1)$$

$$\mathrm{Cd} + \mathrm{SO_2} \xrightarrow{\mathrm{UV}} \text{cyclic } \mathrm{Cd(SO_2)}$$
$$\Delta E = 14 \text{ kcal/mol} \quad (2)$$

B. Anion $M(SO_2)^-$ (M=Zn and Cd)

Laser-ablated zinc atom reactions with SO_2 gave two bands at 1083.9 and 956.1 cm^{-1}, which were wiped out completely with 15 min UV irradiation. On further annealing to 10 K two bands were not recovered. This behavior is due to a typical anion trapped in low temperature matrix. Recalling the similar photochemistry of anions in matrix all absorptions for SMO_2^- were demised with UV irradiation [25].

DOI:10.1063/1674-0068/26/06/747-754

TABLE III Calculated frequencies of M(η^1-OSO)$^-$ (M=Zn and Cd) molecule[a].

	B3LYP				BPW91	Mode description
	^{16}O	^{16,18}O	^{18}O	^{16}O,^{34}S	^{16}O	
Zn(η^1-OSO)$^-$	1083.0(359)	1080.4(325)	1045.5(340)	1070.7(348)	1034.6(329)	S−O antisym str
	955.1(216)	922.1(217)	917.1(185)	946.7(221)	897.3(150)	S−O sym str
	449.4(7)	439.6(7)	429.7(6)	446.2(8)	422.4(5)	S−O sciss
	149.4(86)	143.9(80)	143.6(79)	149.1(86)	157.0(76)	OSO def
	66.8(1)	65.6(1)	65.4(1)	65.9(1)	62.2(1)	OSO def
	37.3(3)	36.9(3)	35.7(3)	37.1(3)	40.2(3)	ZnOSO def
Cd(η^1-OSO)$^-$	1082.6(362)	1079.0(321)	1045.4(341)	1070.0(351)	1034.2(339)	S-O antisym str
	967.2(192)	934.5(200)	928.2(164)	959.0(196)	912.2(125)	S−O sym str
	451.0(7)	441.1(6)	431.2(5)	447.7(7)	424.9(5)	S−O sciss
	138.9(71)	133.2(66)	133.1(65)	138.4(70)	128.1(65)	OSO def
	50.0(2)	49.4(2)	49.1(2)	49.3(2)	46.4(4)	OSO def
	29.8(4)	29.0(4)	28.6(4)	29.6(5)	38.4(2)	CdOSO def

[a] Frequencies in cm^{-1}, intensities (in parentheses) in km/mol.

TABLE IV S−O stretching frequencies and natural charge distributions for M(η^2-O_2S), M(η^1-OSO)$^-$ (M=Zn, Cd, Hg) complexes and SO_2^-.

Molecule or Ion	S−O stretching frequency[a]/cm^{-1}		Natural charge distribution[b]			
	Antisymm	Symm	M	S	O	O
Zn(η^2-O_2S)	980.7 (983.5)	978.6 (972.0)	0.72	1.24	−0.98	−0.98
Zn(η^1-OSO)$^-$	1083.0 (1083.9)	955.1 (956.1)	−0.04	1.10	−0.98	−1.08
Cd(η^2-O_2S)	985.2 (997.4)	976.1 (979.6)	0.73	1.22	−0.98	−0.98
Cd(η^1-OSO)$^-$	1082.6 (1081.7)	967.2 (968.7)	−0.04	1.09	−0.98	−1.07
Hg(η^2-O_2S)	966.0	947.5	0.59	1.23	−0.91	−0.91
Hg(η^1-OSO)$^-$	1081.5	980.2	−0.04	1.08	−1.00	−1.04
SO_2^-	1086.4 (1086.2)	989.5 (990.8)		1.09	−1.05	−1.05

[a] Calculated and observed (in parentheses) S−O stretching frequencies.
[b] Natural charge distributed on the atom.

TABLE V Natural electron configuration for M(η^2-O_2S) (M=Zn, Cd, Hg) complexes.

	Cyclic Zn(SO_2)	Cyclic Cd(SO_2)	Cyclic Hg(SO_2)
S	[core]3S(1.63)3p(2.99)	[core]3S(1.62)3p(3.00)	[core]3S(1.60)3p(3.02)
O	[core]2S(1.85)2p(5.09)	[core]2S(1.85)2p(5.08)	[core]2S(1.85)2p(5.01)
O	[core]2S(1.85)2p(5.09)	[core]2S(1.85)2p(5.08)	[core]2S(1.85)2p(5.01)
M	[core]4S(1.10)3d(9.99)4p(0.19)	[core]5S(1.12)4d(9.99)5p(0.15)	[core]6S(1.34)5d(9.98)5p(0.15)

With $^{34}SO_2$ isotopic substituted sample the two bands shift to 1071.7 and 948.0 cm^{-1}, respectively. With $S^{18}O_2$ sample the correlated bands go to 1046.8 and 918.9 cm^{-1}. With mixed $S^{16}O_2/S^{16,18}O_2/S^{18}O_2$ sample (20%SO_2+40%$S^{16,18}O_2$+40%$S^{18}O_2$) triplet distributions are observed as shown in Fig.1. These observations lead to assigning the bands as the symmetric and antisymmetric stretching vibration modes of S−O in the Zn(SO_2)$^-$ anion. Notice S−O stretching modes for SO_2^- in neon appearing at 1086.2 and 990.8 cm^{-1} [34], which are slightly higher than the same modes for Zn(SO_2)$^-$ anion.

In the reaction of laser ablated Cd and SO_2, two bands at 1081.7 and 969.3 cm^{-1} were found as S−O asymmetry and symmetry stretching vibrations, which shows similar anion behavior. The absorptions due to the Cd(SO_2)$^-$ molecule are identified as a O−S−O antisymmetric stretching mode at 1081.7 cm^{-1} and a O−S−O symmetric stretching mode at 969.3 cm^{-1}. Diagnostic information from isotopic experiments further confirms the assignment. In ^{34}S isotopic experiment, these bands shift to 1069.4 and 961.0 cm^{-1} with the ^{32}S/^{34}S isotope ratio of 1.0115 and 1.0086, respectively. The isotope ratios were quite close to the calculated isotope frequency shift ratio 1.0118 and 1.0086. Unfortunately in the mixed $S^{16}O_2/S^{16,18}O_2/S^{18}O_2$ sample (18%SO_2+45%$S^{16,18}O_2$+37%$S^{18}O_2$) the counterpart bands were rather weak.

DFT frequency calculations were performed for M(SO_2)$^-$ molecules and the results are summarized in

DOI:10.1063/1674-0068/26/06/747-754

Table III. Both B3LYP and BPW91 functionals give very satisfying predictions. With the B3LYP functional the S−O stretching modes for $Zn(SO_2)^-$ were calculated at 1083.9 and 955.1 cm^{-1}, which are almost identical to our observed values in solid neon. Similar excellent predications for $Cd(SO_2)^-$ were made as listed in Table III.

The most likely channel for the formation of $M(SO_2)^-$ (M=Zn, Cd) anions is that neutral $M(SO_2)$ molecule captures laser ablated electrons, as observed previously [25]. With B3LYP functional calculations, the adiabatic electron affinities (energy difference between the ground states of $M(SO_2)$ and $M(SO_2)^-$) are computed around 50 kcal/mol.

$$Zn(SO_2)(^3B_1) + e^- \rightarrow Zn(SO_2)^- \ (^2A)$$
$$\Delta E = -48 \text{ kcal/mol} \quad (3)$$
$$Cd(SO_2)(^3B_1) + e^- \rightarrow Cd(SO_2)^- \ (^2A)$$
$$\Delta E = -49 \text{ kcal/mol} \quad (4)$$

C. Other absorption

The IR spectra observed from the reaction of laser-ablated Zn with SO_2 in neon another band at 976.7 cm^{-1}, which shifted to 965.8 cm^{-1} in $^{34}SO_2$ sample and 936.7 cm^{-1} in $S^{18}O_2$ sample, also distinctly increased on the 15 min UV light irradiation and then recovered on annealing to 10 K. Unfortunately the isotope frequency shifts were not clear enough to be assigned to each vibration mode. In the mixed $SO_2/S^{16,18}O_2/S^{18}O_2$ experiment, adsorption at 974.8, 943.7, and 940.8 cm^{-1} also showed the analogous change. But in the spectra with pure SO_2 and $^{34}SO_2$, it was hardly to find out the same group to attribute them. The similar adsorption in argon matrix appeared at 980.1, 975.1, and 945.8 cm^{-1} with the $SO_2/S^{16,18}O_2/S^{18}O_2$ mixture. In the reaction of Cd and SO_2 in neon and argon, the IR spectra showed weak bands at 987.6 and 985.3 cm^{-1} respectively, which decreased 30% on 15 min UV irradiation. The spectra meanwhile show the $^{32}S/^{34}S$ isotope frequency shifts. However, in the $SO_2/S^{16,18}O_2/S^{18}O_2$ mixed sample reaction with Cd, analogous shifts were scarcely observed.

D. Bonding

DFT calculations indicate that the M(η^2-O_2S) molecules found in the triplet ground state are more stable than the singlet. The natural charge distributions of Zn(η^2-O_2S) for metal center Zn is 0.72 a.u. while the charges for O, S are −0.98 and 1.24 a.u., respectively. For Cd(η^2-O_2S) the metal center is 0.73 a.u. while the charges for O and S are −0.98 and 1.22 a.u. (Table IV). They both indicate that charge transfer occurs from metal to SO_2 subunit. Natural electron configuration for M(η^2-O_2S) molecules are listed in Table V. As expected one electron transfers from s orbitals of zinc or cadmium metal atom to SO_2 ligand. In our experiments absorptions for M(η^2-O_2S) molecules were observed very weakly on deposition but increased markedly on UV irradiation, suggesting UV irradiations induce the charge transfer from metal to SO_2, and ionic pair $M^+(SO_2^-)$ was trapped in low temperature matrix. Figure 6 illustrates the singlet and triplet PES along the dissociation paths, which show that triplet M(η^2-O_2S) is less stable than the ground state metal atoms and SO_2. However the ionic pair M(η^2-O_2S) is located in the lowest energy on triplet PES, which can be kinetically stabilized in low temperature matrix.

The symmetric and antisymmetric S−O stretching modes of $Zn^+SO_2^-$ were observed at 972.0 and 983.5 cm^{-1}, which are much lower than the same modes identified for SO_2^- anion, indicating strong interaction of SO_2^- subunit with Zn^+. Calculations show that the O−S−O bond angle for Zn(η^2-O_2S) complex is 10° smaller than the same angle for SO_2^- anion (Fig.5). Furthermore the Zn−O bond distance is 2.131 Å, suggesting covalent bond formed between zinc and oxygen of SO_2. Based on the charge transfer character this bond can be described as a polarized covalent bond. The observed S−O stretching frequencies for Cd(η^2-O_2S) are close to the same modes for Zn(η^2-O_2S). Also the calculated structure is very similar, as shown in Fig.5, so the bond character is the same.

It is interesting to compare the geometric structure, natural charge distributions and stability of Hg(η^2-O_2S) with Zn(η^2-O_2S) and Cd(η^2-O_2S). As shown in Fig.5 and Table IV, the geometric parameters and charge distributions for Hg(η^2-O_2S) complex are close to that of Zn(η^2-O_2S) and Cd(η^2-O_2S), however, the formation of Hg(η^2-O_2S) is very endothermic. Based on CCSD(T) energy calculation, the reaction of mercury atom with SO_2 to give cyclic $Hg(SO_2)$ is endothermic by 42 kcal/mol (Reaction (5)), which is much higher than the same reactions for zinc and cadmium (Reactions (1) and (2)). The cyclic $Hg(SO_2)$ molecule was not observed in our low temperature matrix experiments, which is in agreement with the calculated high endothermic reaction (5). The absence of Hg(η^2-O_2S) complex can be understood by taking into account the relativistic effect that resulted in the contraction of 6s valence shell and the ionization potential is higher for Hg than that for Zn and Cd. As shown in Table V the electron transfer from Hg to SO_2 is much less than that of Zn and Cd. For "ion pair" Hg(η^2-O_2S) complex the σ type donation from SO_2^- subunit to s orbital of Hg^+ is extremely weak, which cannot contribute stabilization energy.

$$Hg + SO_2 \rightarrow \text{cyclic } Hg(\eta^2\text{-}O_2S)$$
$$\Delta E = 42 \text{ kcal/mol} \quad (5)$$

The "ion pair" M(η^2-O_2S) complexes have very high electron affinity (Reactions (3) and (4)). The natural charge distributions of Zn(η^1-OSO)$^-$ for metal center is −0.04 a.u. (Zn) while the charges for O, S are around

DOI:10.1063/1674-0068/26/06/747-754

−1 and 1 a.u., respectively. Similar charge distributions were found for Cd(η^1-OSO)$^-$. This result clearly shows the valence orbitals of Zn and Cd are full, and the anions M(η^1-OSO)$^-$ favor η^1 type bonding. Recall the sulfur dioxide complexes with alkali and alkaline earth metals giving η^2-O,O fashion molecules [21, 35, 36].

V. CONCLUSION

The cyclic structure M(η^2-O_2S) (M=Zn and Cd) with a C_{2v} symmetry was proposed as the most stable configuration in laser-ablated zinc and cadmium atom reaction with SO_2 in excess neon. Another product M(η^1-OSO)$^-$ was inverted into M(η^2-O_2S) after full mercury arc irradiation. The appropriate $^{34}SO_2$ and $S^{16,18}O_2$ isotope shifts support the assignment. DFT (B3LYP and BPW91) frequency calculations reproduce the IR spectra of these molecules very well. The data came out to the conclusion that electron transfer from Zn and Cd atoms to the SO_2 molecule reduced the value of the O−S−O angle and made the S−O bonds weaker. Meanwhile, strong polarized covalent bond formed between metal atoms and oxygen of SO_2.

VI. ACKNOWLEDGMENTS

This work was supported by the National Natural Science Foundation of China (No.21173158 and No.21373152).

[1] L. Y. Wu, S. R. Tong, W. G. Wang, and M. F. Ge, Atmos. Chem. Phys. **11**, 6593 (2011).
[2] J. A. Rodriguez, T. Jirsak, L. Gonzalez, J. Evans, M. Perez, and A. Maiti, J. Chem. Phys. **115**, 10914 (2001).
[3] P. Liu and J. A. Rodriguez, J. Chem. Phys. **119**, 10895 (2003).
[4] L. Giakoumelou, V. Parvulescu, and S. Boghosian, J. Catal. **225**, 337 (2004).
[5] X. F. Wang, L. Andrews, and C. J. Marsden, Inorg. Chem. **48**, 6888 (2009).
[6] X. F. Wang and L. Andrews, J. Phys. Chem. A. **113**, 8934 (2009).
[7] H. Sellers and E. Shustorovich, J. Mol. Catal. A **119**, 367 (1997).
[8] A. Decken, C. Knapp, G. B. Nikiforov, J. Passmore, J. M. Rautiainen, X. P. Wang, and X. Q. Zeng, Chem. Eur. J. **15**, 6504 (2009).
[9] K. Gleu, W. Breuel, and K. Rehm, Z. Anorg. Allg. Chem. **235**, 201 (1938).
[10] K. Gleu and W. Breuel, Z. Anorg. Allg. Chem. **235**, 211 (1938).
[11] D. M. P. Mingos, Transition Met. Chem. **3**, 1 (1978).
[12] D. C. Moody, R. R. Ryan, and G. J. Kubas, Abstr. Pap. Am. Chem. S. **179**, 34 (1980).
[13] W. A. Schenk, Angew. Chem. Int. Ed. Engl. **26**, 98 (1987).
[14] J. K. Shen, G. J. Kubas, and A. L. Rheingold, Inorg. Chim. Acta **240**, 99 (1995).
[15] J. S. S. Harter, M. L. Campbell, and R. E. McClean, Int. J. Chem. Kinet. **29**, 367 (1997).
[16] R. E. McClean and L. Norris, Phys. Chem. Chem. Phys. **7**, 2489 (2005).
[17] J. Petersen, E. Lork, and R. Mews, Chem. Commun. 2593 (1996).
[18] R. Mews, E. Lork, P. G. Watson, and B. Gotler, Coord. Chem. Rev. **197**, 277 (2000).
[19] D. E. Milligan and M. E. Jacox, J. Chem. Phys. **55**, 1003(1971).
[20] M. Allavena, R. Rysnik, D. White, V. Calder, and D. E. Mann, J. Chem. Phys. **50**, 3399 (1969).
[21] L. Bencivenni, F. Ramondo, and R. Teghil, Inorg. Chim. Acta. **121**, 207 (1986).
[22] P. Benndorf, S. Schmitt, R. Koppe, P. Ona-Burgos, A. Scheurer, K. Meyer, and P. W. Roesky, Angew. Chem. Int. Ed. **51**, 5006 (2012).
[23] G. J. Kubas, Inorg. Chem. **18**, 182 (1979).
[24] X. Liu, X. F. Wang, Q. Wang, and L. Andrews, Inorg. Chem. **51**, 7415 (2012).
[25] X. Liu, X. F. Wang, Q. Wang, and L. Andrews, Phys. Chem. Chem. Phys. **15**, 9823 (2013).
[26] L. J. Tong, Q. Wang, X. Liu, and X. F. Wang, Chem. Phys. Lett. **574**, 18 (2013).
[27] M. J. Frisch, G. W. Trucks, H. B. Schlegel, G. E. Scuseria, M. A. Robb, J. R. Cheeseman, J. A. Jr. Montgomery, T. Vreven, K. N. Kudin, J. C. Burant, J. M. Millam, S. S. Iyengar, J. Tomasi, V. Barone, B. Mennucci, M. Cossi, G. Scalmani, N. Rega, G. A. Petersson, H. Nakatsuji, M. Hada, M. Ehara, K. Toyota, R. Fukuda, J. Hasegawa, M. Ishida, T. Nakajima, Y. Honda, O. Kitao, H. Nakai, M. Klene, X. Li, J. E. Knox, H. P. Hratchian, J. B. Cross, V. Bakken, C. Adamo, J. Jaramillo, R. Gomperts, R. E. Stratmann, O. Yazyev, A. J. Austin, R. Cammi, C. Pomelli, J. W. Ochterski, P. Y. Ayala, K. Morokuma, G. A. Voth, P. Salvador, J. J. Dannenberg, V. G. Zakrzewski, S. Dapprich, A. D. Daniels, M. C. Strain, O. Farkas, D. K. Malick, A. D. Rabuck, K. Raghavachari, J. B. Foresman, J. V. Ortiz, Q. Cui, A. G. Baboul, S. Clifford, J. Cioslowski, B. B. Stefanov, G. Liu, A. Liashenko, P. Piskorz, I. Komaromi, R. L. Martin, D. J. Fox, T. Keith, M. A. Al-Laham, C. Y. Peng, A. Nanayakkara, M. Challacombe, P. M. W. Gill, B. Johnson, W. Chen, M. W. Wong, C. Gonzalez, and J. A. Pople, *Gaussian 03, Revision D.01*, Wallingford CT: Gaussian, Inc., (2004).
[28] A. D. Becke, J. Chem. Phys. **98**, 5648 (1993).
[29] C. Lee, Y. Yang, and R. G. Parr, Phys. Rev. B **37**, 785 (1988).
[30] M. J. Frisch, J. A. Pople, and J. S. Binkley, J. Chem. Phys. **80**, 3265 (1984).
[31] A. D. Becke, Phys. Rev. A **38**, 3098 (1988).
[32] A. D. Becke, J. Chem. Phys. **107**, 8554 (1997).
[33] K. Raghavachari, J. S. Binkley, R. Seeger, and J. A. Pople, J. Chem. Phys. **72**, 650 (1980).
[34] D. Forney, C. B. Kellogg, W. E. Thompson, and M. E. Jacox, J. Chem. Phys. **113**, 86 (2000).
[35] F. Ramondo and L. Bencivenni, Mol. Phys. **67**, 707 (1989).
[36] A. Goumri, D. Laakso, J. D. R. Rocha, E. Francis, and P. Marshall, J. Phys. Chem. **97**, 5295 (1993).

DOI:10.1063/1674-0068/26/06/747-754